The fronto-parietal network connects more strongly to central than peripheral V1

Sara Sims[1], Pinar Demirayak[2], Simone Cedotal[2], & Kristina Visscher[2]
1 University of Alabama Department of Psychology, 2 University of Alabama Department of Neurobiology

ABSTRACT

Central and peripheral vision are important for distinct aspects of everyday life. We use central vision to read and peripheral vision to get the gist of a scene. To understand how these differences are reflected in connectivity between V1 and higher-order cognitive areas, we examined the differential connectivity of V1 that represent central and peripheral vision. We used diffusion-weighted-imaging and resting-state blood-oxygen-level-dependent data to examine structural and functional connectivity. The present results demonstrate strong evidence that centrally-representing portions of V1 are more strongly functionally and structurally connected to the fronto-parietal network than are peripherally representing portions of V1. This suggests that these patterns of connections between central V1 and the fronto-parietal network are direct and support attention-demanding visual tasks. Overall, our findings contribute to understanding how the human brain processes visual information and forms a baseline for any modifications in processing that might occur with training or experience.

Keywords: V1, structural connectivity, functional connectivity, visual eccentricity, functional networks

INTRODUCTION

The functionality of central vision is different from peripheral vision. Central vision is used for fixation and has a higher acuity that makes it useful for tasks such as reading and object identification (Larson & Loschky, 2009; Pelli et al., 2007; Trouilloud et al., 2020; Yoo & Chong, 2012). The majority of the visual field comprises peripheral vision, which has lower acuity but is responsible for visual tasks such as visual search and getting the gist of a scene (Larson & Loschky, 2009; Rosenholtz, 2016; Trouilloud et al., 2020). However, differences in acuity between peripheral and central vision alone do not provide a full explanation of the extent of disparity in visual ability with different eccentricities (Levi, Klein, & Aitsebaomo, 1985; Levi, Klein, & Wang, 1994). Information processing of central and peripheral visual information also differ. Peripheral visual information is processed faster than central information (Lu, Lesmes, & Dosher, 2002) which helps determine the salience of objects within the visual field and enables the visual system to direct saccades, fast eye movements, to a salient location (Lu et al., 2002). When central vision is oriented to the salient location, it provides high acuity information and distinguishes it from competing, distracting information (Lu et al., 2002).

Human primary visual cortex (V1) is organized along the calcarine sulcus in a progression of posterior central representing regions (central V1) to anterior peripheral representing regions (far-peripheral V1) (Duncan, Sample, Weinreb, Bowd, & Zangwill, 2007; Engel, Glover, & Wandell, 1997; Fox, Miezin, Allman, Van Essen, & Raichle, 1987). The anatomical regions representing central and peripheral V1 differ in their cortical thickness (Burge et al., 2016). The central representing portion of V1, or the part of the visual field that is being used for fixation, has a thicker cortex compared to the peripheral representing cortex in individuals with healthy vision (Burge et al., 2016).

There has been extensive prior research into the physiological differences between central and peripheral V1. Encoding of visual information differs within V1 representations of central and peripheral visual fields. V1 is disproportionately devoted to processing central visual field derived visual information. The over-representation of central visual information leaves the majority of the visual field, peripheral vision, under-represented in V1. In other words, the magnification factor (mm per degree of visual angle) is greater for central vision than peripheral vision (To, Gilchrist, Troscianko, & Tolhurst, 2011). Also reflecting over-representation, receptive field size is greater for neurons in peripheral V1 than neurons in central V1 (Hubel & Wiesel, 1974).

Central and peripheral V1 also differ in how higher-order processing areas modulate their responses. Functional properties of cortical neurons are adaptive; their responses are influenced by top-down demands of high-order cognitive processing tasks (Gilbert & Li, 2013). For example, attention and expectation are top-down processes (i.e. high-order cognitive functions) that influence visual information processing during behavioral tasks (Gandhi, Heeger, & Boynton, 1999; Somers, Dale, Seiffert, & Tootell, 1999; Tootell et al., 1998; Yeshurun & Carrasco, 1998). This top-down control is different for central vs. peripheral vision. Attention influences the spatial summation of receptive fields so that spatial summation in foveal cells decreases and spatial summation in the peripheral cells in the V1 area increases (Roberts, Delicato, Herrero, Gieselmann, & Thiele, 2007). Further, psychophysiological data demonstrates that top-down influences on central vision stimuli are stronger than on peripheral vision stimuli (Chen & Treisman, 2008; Zhaoping, 2017). Similarly, attentional suppression of distractors is greater for central vision than peripheral vision (Chen & Treisman, 2008). Overall, there appears

to be an important distinction in higher-order cognitive operations between central and peripheral vision processing. These cognitive operations are thought to involve interactions between sensory brain networks with higher-order brain networks (eg. (Casarsa De Azevedo, 2019; Furl, 2015; Gazzaley et al., 2007; Griffis, Elkhetali, Burge, Chen, & Visscher, 2015; Mantini, Corbetta, Perrucci, Romani, & Del Gratta, 2009; McMains & Kastner, 2011; Yeshurun & Carrasco, 1998).

Resting-state functional networks are groups of brain regions whose activity tends to be temporally correlated at rest (Zalesky, Fornito, Cocchi, Gollo, & Breakspear, 2014). One way a functional network can be identified is through clusters of correlated activity in the cortex (Yeo et al., 2011). The fronto-parietal network (FPN) directs attentional control (e.g., (Zanto & Gazzaley, 2013), the cingulo-opercular network (CON) supports the maintenance of task demands (e.g., (Coste & Kleinschmidt, 2016), and the default mode network (DMN) is less active when there are attentional or task goals (e.g., (Raichle, 2015) and instead supports tasks such as memory retrieval and semantic processing (Binder, 2012; Gerlach, Spreng, Gilmore, & Schacter, 2011; Sestieri, Shulman, & Corbetta, 2010; Spreng, 2012). Since functional networks can influence visual information processing in different ways, networks likely differ in how they connect to representations of the visual field across V1. There are also feedforward connections between V1 and functional network regions, as evidenced by the fact that strong stimulus-driven signals are observed in higher-order brain regions (Katsuki & Constantinidis, 2014).

Previous work in our lab has investigated how the central-to-peripheral cortical organization of V1 influences functional connectivity between V1 and the rest of the cortex (Griffis et al., 2017). This prior work indicated that there were retinotopic patterns of functional connectivity between V1 and functional networks during resting fixation. Specifically, the central representing portion of V1 was more functionally connected to regions belonging to the FPN and the far-peripheral representing portion of V1 was more functionally connected to regions belonging to the DMN. The fact that, as described above, central vision is under different top-down control than peripheral vision, might underlie its preferential connection to the FPN which is related to directing attentional control and has been shown to facilitate bottom-up and top-down attentional processes for visual information (Katsuki & Constantinidis, 2014). The role of far-peripheral vision in environmental monitoring and the need for suppression of visual information from this portion of the visual field during central fixation might be the reason for preferential connectivity to the task-negative DMN (Li, 2002). However, our previous work was limited by a small sample size (i.e., 20 participants) and design (i.e., data were acquired during the resting fixation blocks of a visual task) issues (Griffis et al., 2017). These limitations leave questions regarding whether previous functional findings extend to free viewing during rest in a larger sample and, critically, how these effects relate to differences in the anatomical (i.e. white matter) connections of central vs. peripheral V1.

Anatomical connections can be examined by an invasive method in which retrograde or anterograde tracers are injected into the brain and resulting staining of brain regions are examined. These types of studies inject one location and look for staining in other locations, and this can give fine detail information about the connection patterns of the brain (e.g. (Felleman & Van Essen, 1991). Because of the slow and arduous nature of these studies, examinations of connections from visual regions have been primarily focused on defining structural connectivity across areas thought to be primarily involved with vision (Andersen, Asanuma, Essick, & Siegel, 1990; Lysakowski, Standage, & Benevento, 1988; Neal, Pearson, & Powell, 1990). Thus, it is

not clear whether prior work did not find connections between V1 and higher-order processing areas or simply did not report those findings from their analysis. A more comprehensive study aimed to close this gap in the literature by creating a connectivity matrix throughout the whole cerebral cortex in macaque (Markov et al., 2014). An injection of anterograde tracer was placed into central-representing V1. Connections that projected from V1 to regions of the frontal and parietal cortex were found including: F5 (involved in motor planning), 8l (frontal eye fields), and 7A (involved in attention modulation and planning) (Markov et al., 2014). Of the frontal and parietal regions which were examined by Markov et. al, only area 8l (frontal eye fields) showed top-down connections to V1. Importantly, in the taxonomy put forward by Yeo (2011), the "fronto-parietal network" does not overlap with frontal eye fields (instead the frontal eye fields are within the Dorsal Attention Network) (Glasser et al., 2016; Wang, Mruczek, Arcaro, & Kastner, 2015). No tracer was injected into the peripheral representing portion of V1. Thus, it is not clear whether these V1-fronto-parietal connections exist for peripheral portions of V1.

While brain anatomy is relatively fixed in adulthood, a healthy brain changes the structural connections between regions with experience and age (Davis et al., 2009). White matter tracts correspond to direct connections between brain regions. Structural connections can be studied in-vivo in humans with diffusion-weighted MRI and tractography. Major white matter tracts that connect to the occipital lobe such as the inferior fronto-occipital fasciculus (connects occipital lobe to lateral prefrontal cortex) and the inferior longitudinal fasciculus (connects occipital lobe to anterior temporal lobe) have been well documented using tractography methods in humans. However, the inferior fronto-occipital fasciculus has not been found in the macaque brain, which may explain why tracer studies investigating V1 have not helped to inform occipital-prefrontal cortex connections (Takemura et al., 2016).

The goals of the current study are (1) to assess the reproducibility and generalizability of retinotopic effects on functional connections between V1 and functional networks, found in prior work (Griffis et al., 2017)), in a new dataset collected under different task conditions (previous work used blocks of rest during a task with central fixation and the current data was collected as part of a resting-state only scan), (2) extend this prior work to the retinotopic effects of structural connections between V1 and functional networks, and (3) examine the relationship between these functional and structural connections. Since functional connectivity between two brain regions could come from both direct and indirect structural connections, we used DWI to examine direct connections between regions (Adachi et al., 2012; Honey et al., 2009) that were previously found to show functional connections.

To address these goals, we used resting-state BOLD fMRI and DWI to examine if portions of V1 that represent different visual eccentricities differ in their functional and structural connectivity to functional networks. We found 1) strong evidence that centrally representing portions of V1 are more strongly functionally connected to the frontoparietal network than are peripherally representing portions of V1, 2) Structural connections show the same pattern, with stronger connections between central V1 and frontoparietal regions, in particular a lateral frontal portion of the frontoparietal network, and 3) the pattern of structural and functional connections is similar, suggesting that this lateral frontal connection pattern arises from a direct connection, rather than from an indirect connection.

METHODS

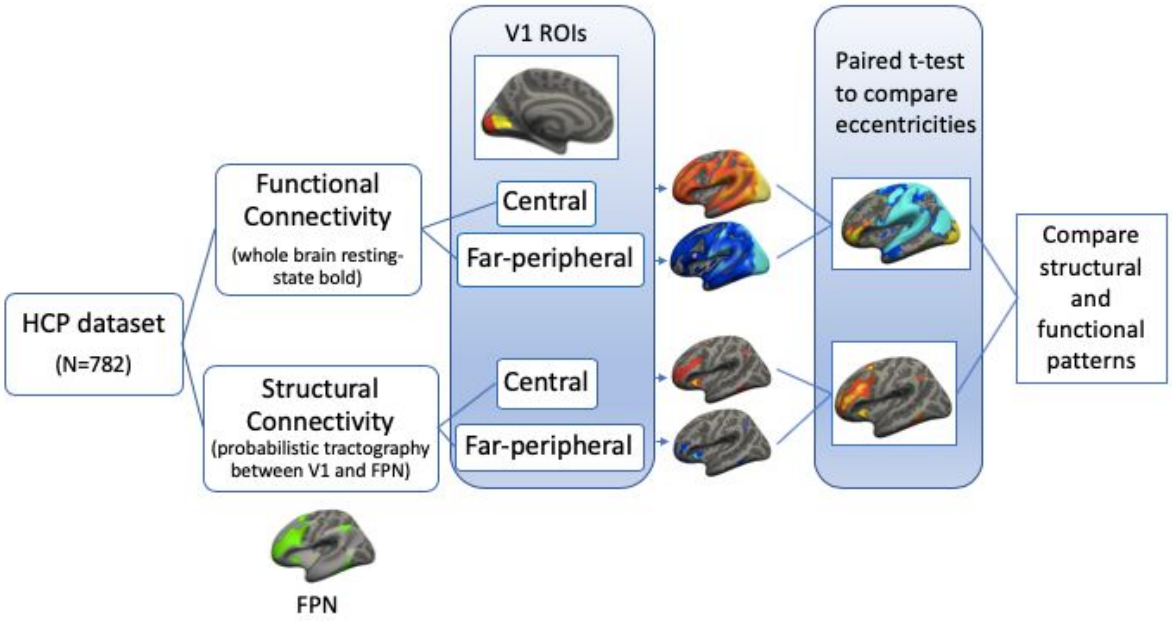

Figure 1. Graphical representation of methods. *Moving from left to right: data from the HCP dataset through the analysis stream and representations of the results. The top portion shows the analyses for functional connectivity and the bottom portion shows the analysis for structural connectivity. These analysis streams are largely parallel.*

Participants

Diffusion weighted imaging, resting-state functional imaging, and structural imaging data from the 900-subject release of the Human Connectome Project (HCP) dataset were used in the study (Figure 1). Participants in this dataset were healthy young adults between 22-36 years of age who had normal or corrected-to-normal vision. Most subjects had at least one relative in the group, many of them are twins. Our hypotheses are not about individual differences, and due to the large sample size of the data there is still a great deal of diversity in the sample, therefore we did not treat related and unrelated samples separately. Using a relatively large sample size has the advantage of facilitating replication and extension of findings for the researchers. Participants with structural abnormalities (e.g. tumors and large area brain damage) that were identified through HCP quality control were excluded from the study. We then visually inspected the remaining data for white matter abnormalities. Participants were excluded if their structural scans displayed large or punctate white matter hyperintensities that were easily detected by eye. In total, 114 subjects were excluded from the original 900 subject dataset. Seven hundred eighty-six healthy subjects passed quality control standards which included 335 males and 449 females. fMRI data from four of them were dropped due to quality standards for functional comparison. Otherwise, the same participants were used in both structural and functional connectivity analyses.

Data Acquisition

T1-weighted structural MRI, resting state fMRI and multi-shell diffusion weighted (DWI) MRI data were acquired using a customized Siemens 3T "Connectome Skyra" (Sotiropoulos et al., 2013). High-resolution three-dimensional MPRAGE, T1-weighted anatomical images (TR = 2400 ms, TE = 2.14 ms, flip angle = 8, FOV = 320 x 320 mm^2, voxel size 0.7 x 0.7 x 0.7 mm^3, number of slices = 256, acceleration factor (GRAPPA) = 2) were used. Functional magnetic resonance imaging (fMRI) data were acquired with a multi-band gradient echo (GE) EPI sequence (voxel size = 2 x 2 x 2 mm^3; TR= 720 ms; TE = 33.1 ms; flip angle = 52 degrees; FOV = 208 x 180 mm^2; number of slices = 72) in four runs (each of them took approximately 15 minutes) with eyes open and related fixation on a cross on a dark background. Phase encoding direction was obtained in right-to-left for half of the scans and in left-to-right for the other half of the resting-state scans.

For DWI, multi-band diffusion-weighted echo-planar (EP) images (voxel size = 1.25 x 1.25 x 1.25 mm^3; TR= 5520 ms; TE = 89.5 ms; flip angle = 78 degrees; MB = 3; FOV = 210 x 180 mm^2; number of slices = 111; b=1000, 2000 and 3000 s/mm^2, diffusion directions = 95, 96 and 97) were used. DWI data includes six runs (each of them took approximately 9 minutes and 50 seconds). Each gradient table was acquired with right-to-left and left-to-right phase encoding polarities which were then merged after distortion correction as part of the HCP Preprocessing Pipeline (Glasser et al., 2013).

V1 Eccentricity Segment Definitions

V1 eccentricity segments were hand-drawn within the Freesurfer fsaverage V1 label as described in a previous publication from our lab (Burge et al., 2016; Griffis et al., 2017, 2015). Nine segments of V1, approximately 10mm wide were created for both the left and right hemisphere of the Freesurfer fsaverage brain. The V1 segments were then transformed from fsaverage space to individual anatomical space, producing subject-specific segmentation of V1. Previous work has shown that cortical anatomy is a reliable predictor of the retinotopic organization of V1 (O. Hinds et al., 2009; O. P. Hinds et al., 2008) so that the more posterior parts of the visual cortex represent more central portions of the visual field. The average eccentricity of each segment was estimated from Benson and colleagues' probabilistic retinotopy template (Benson et al., 2012) and 3 retinotopic regions were identified: central vision (mean eccentricity estimates of 0-2.2 degrees visual angle), mid-peripheral vision (mean eccentricity estimates of 4.1-7.3 degrees visual angle) and far-peripheral vision (mean eccentricity estimates of 14.1-25.5 degrees visual angle) (Figure 2). These ROIs were defined in the gray matter on the cortical sheet for the freesurfer template, then moved into the individual anatomical space for each participant. To avoid the potential for artifacts due to differences in ROI size, the number of segments per eccentricity region were assigned to more evenly distribute ROI size. The 'central vision' ROI included three segments, while mid-peripheral and far-peripheral regions included two segments each to keep the number of vertices similar between sections.

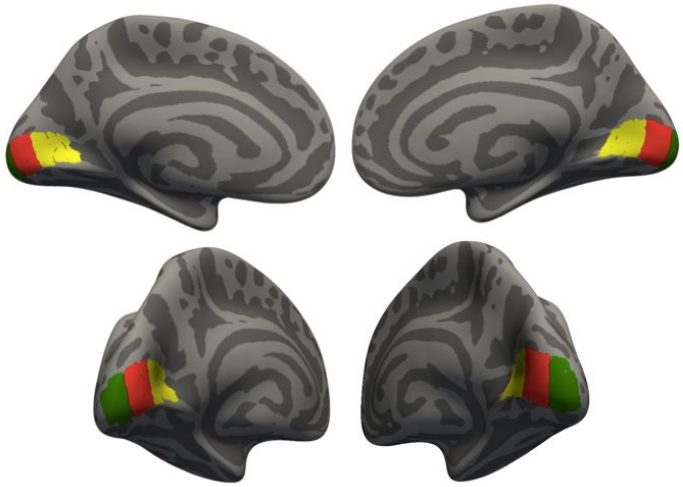

Figure 2. V1 Eccentricity segments. The Far-peripheral representing section of V1 is shown in yellow, the mid-peripheral representing section of V1 is shown in red, and the central representing section of V1 in green. These regions of V1 were used as target regions for tractography analyses and seed regions in functional connectivity analyses. For brevity, we sometimes use shorthands like "central V1" to refer to these centrally-representing regions.

Functional Network ROI Definitions

FP, CO, and DMN labels created by (Yeo et al., 2011) were transformed from the Freesurfer fsaverage brain to individual anatomical space (Yeo et al., 2011). Voxels within the grey matter corresponding to the network ROIs were used as seed voxels for the functional connectivity analysis and voxels within the white matter corresponding to the network ROIs were used as track seeds. Voxels were identified using the Freesurfer mri_aparc2aseg command and then transformed into individual diffusion space.

Data Analysis

Resting-State Scan Image Preprocessing

The HCP minimal preprocessing pipeline that includes artifact removal, motion correction, and registration to standard space was used (Glasser et al., 2013). Along with the preprocessing steps already described by Glasser and colleagues (2013), additional preprocessing steps were performed on the residual BOLD data to reduce spurious variance not associated with neural activity as described in this paragraph. Functional images were censored for movement according to validated techniques (Carp, 2013; Griffis et al., 2017; Power, Barnes, Snyder, Schlaggar, & Petersen, 2012). Time points in which a participant moved more than 0.5 mm in one TR were replaced with an interpolated image from adjacent images. Runs were excluded if mean framewise displacement across the run was greater than 3 mm in any direction. Temporal band-pass filtering was applied between 0.009 and 0.08 Hz. In order to reduce artifactual noise, we applied regressors, including white matter and CSF signals and motion parameters that were extracted during motion correction for each subject from the previous step. Surface reconstruction, the region of interest (ROI) label generation, and image registration were also visually inspected for all subjects to ensure the accuracy of these automated computations. Next, right-to-left and left-to-right acquisitions were concatenated into a single 4D volume for the functional connectivity analysis.

Functional Connectivity Analysis

Functional connectivity refers to synchronization between time courses of activation between two brain areas due to the similar temporal signal profiles from these connected areas (Friston, Holmes, Poline, Frith, & Frackowiak, 1995). Correlation maps for each participant were obtained from seed-to-voxel connectivity measurements between central, mid-peripheral, and far-peripheral ROIs within the primary visual cortex (V1) to each voxel in the brain. The resulting correlation coefficient maps were converted to z-score maps using Fisher's z transform. Fischer's transformed z-score maps were projected onto the individual cortical surface from 1mm below the white/gray matter boundary using Freesurfer's mri_vol2surf command. To test the functional connectivity differences, difference maps were compared by paired t-test using Freesurfer's mri_glmfit function.

Diffusion-weighted Image Preprocessing

The HCP minimal preprocessing pipeline was used for correction for B_0 and eddy current distortions (Glasser et al., 2013). Further DWI data preprocessing was performed using the FMRIB's Diffusion Toolbox (FDT v3.0) using GPU for the acceleration of processing (graphics processing unit) (Hernández et al., 2013; Robinson et al., 2018). For each voxel, a distribution of diffusion parameters was estimated by means of Markov Chain Monte Carlo sampling, which also allows for crossing fiber orientations (Behrens, Johansen-Berg, Jbabdi, Rushworth, & Woolrich, 2007).

Tractography

The results from our previous study on functional connectivity, replicated here, led to the hypothesis that structural connections from central vs. peripheral regions would differ between the FP, CO, and DMN networks. Thus, we used these network regions as seeds in probabilistic tractography performed by FMRIB's Diffusion Toolbox (FDT) (Hernandez-Fernandez et al., 2019) and used the V1 ROIs as targets. For each seed voxel, 10,000 streamlines (along with default settings of maximum steps: 2000, step length: 0.5mm, curvature threshold: 0.2) were initiated and separate samples of the voxelwise diffusion distribution were calculated. A distance correction and loop-check, which prevents circular pathways, were applied. The tractography then resulted in each voxel within the seed ROI containing the number of streamlines that reached the target (V1 region) from that voxel. Tracking was performed in individual diffusion space. Seed and target regions were transformed into diffusion space for tractography analysis and tractography results were transformed into individual anatomical Freesurfer space for visualization.

Track frequencies (number of streamlines that reached the target) were transformed into track probabilities (likelihood of a track reaching the target) by dividing the log-scaled track frequency by the maximum log-scaled track frequency (Beer, Plank, & Greenlee, 2011; Wirth, Frank, Greenlee, & Beer, 2018). This was done to mitigate possible biases arising from size differences of seeds (Smith, Beer, Furlan, & Mars, 2018; Wirth et al., 2018). Track probabilities were projected onto the individual cortical surface from 1mm below the white/gray matter boundary using Freesurfer's mri_vol2surf command (Beer et al., 2011; Wirth et al., 2018). Surface maps of the track termination probabilities were smoothed using a $2mm^2$ Gaussian filter and averaged across all subjects.

Tractography Analysis

To test the hypothesis that patterns of functional connections previously found in V1 (Griffis et al., 2017) are similar to patterns of structural connections, comparisons were made between the central and far-peripheral eccentricity segments of V1 connectivity patterns to the FPN. Differences in track probabilities corresponding to V1 eccentricity segments connections were compared by paired t-test (using Freesurfer's mri_glmfit).

Comparison of Functional and Structural Connectivity

A subject-wise Pearson's correlation coefficient was performed for comparison across participants' structural connections and functional connections of central V1 eccentricity segment and 3 functional resting-state networks (FPN, CON, DMN).

RESULTS

We hypothesized that the connectivity between the eccentricity segments of primary visual cortex (V1) and functional networks (i.e., FPN, CON, DMN) differs in both structural and functional connections. We compared spontaneous BOLD activity within the same ROI and we performed probabilistic tractography for the comparison of structural connections.

Functional Connections to V1 depend on Eccentricity

We compared the whole-brain functional connectivity patterns of each segment of V1-central, mid-peripheral, and far-peripheral. The t-test comparing functional connectivity to different eccentricity segments in V1 revealed significant effects ($p<.001$) and brain regions belonging to FP, CO, and DMN functional networks (Figure 3). Notably, central representing V1 was preferentially connected (over mid-peripheral and far-peripheral V1) to regions associated with the FP network, including the mid orbitofrontal and inferior parietal regions of the FP network. While mid and far-peripheral representing V1 were not preferentially connected (over central V1) to any specific networks (Baldassano, Fei-Fei, & Beck, 2016). This finding is similar to those found in a previous publication from our lab (Griffis et al., 2017). Those previous results had also shown differences in connectivity between mid-peripheral-representing regions and far-peripheral representing regions, which were not observed here, (Figure 3). Thus, in this paper, we focus on distinctions between centrally-representing portions of V1 to far-peripheral portions of V1.

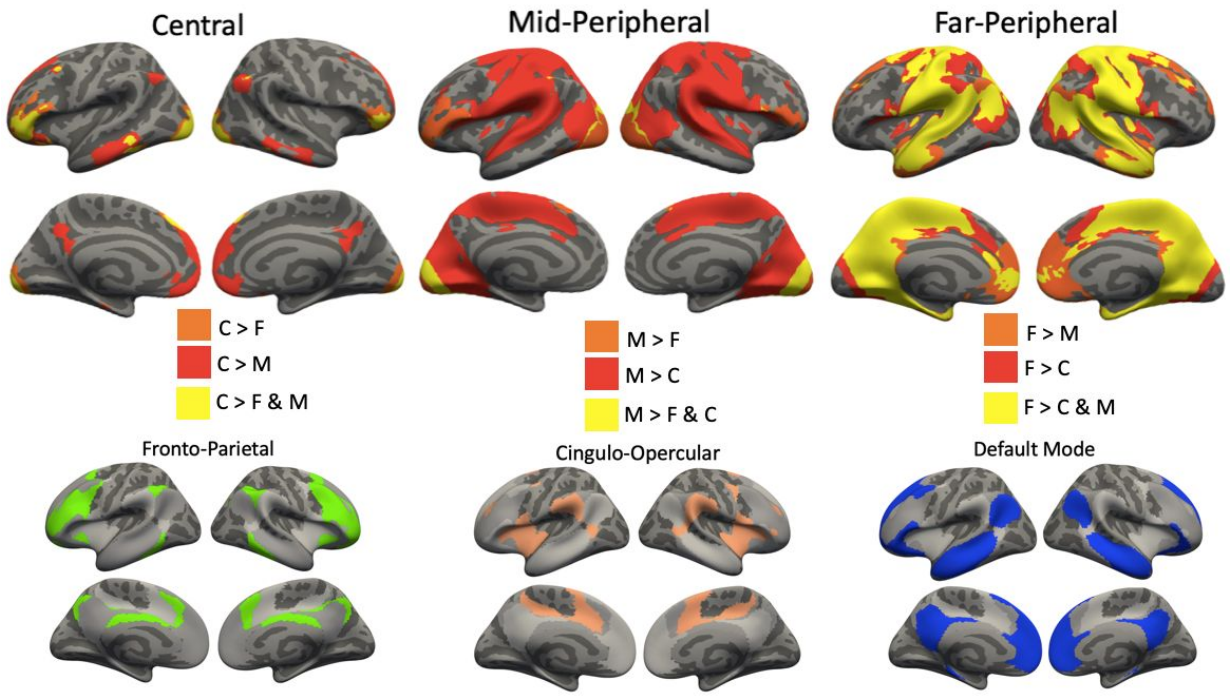

Figure 3. Comparisons of functional connectivity between V1 eccentricity segments and homology to known resting-state networks. *Top Row:* Differences in Functional Connectivity depending on eccentricity. The far left panel highlights vertices which show significantly stronger connections to central V1 than other portions of V1. There, vertices in yellow showed stronger (z>3) connectivity to central V1 than to both Far peripheral and mid-peripheral regions. Red indicates stronger connectivity to Central than Mid-peripheral regions, and orange indicates stronger connectivity to Central than Far-peripheral regions. The middle and right panels show analogous images highlighting vertices with significantly stronger connections to mid-peripheral and far-peripheral regions. For the middle panel, red is where mid-peripheral is greater than central and orange is where mid-peripheral is greater than far-peripheral. For the panel on the right, red is where far-peripheral is greater than central and orange is where far-peripheral is greater than mid-peripheral. Inferences regarding functional connectivity are based on these maps.
Bottom Row: Functional Networks for comparison to the top-row. Previously documented FPN, CON, and DMN (from Yeo et al., 2011). The FPN is shown in green, the CON is shown in tan, and the DMN is shown in blue. Note homologies between the FP network and the left panel.

To directly compare central and peripheral V1 functional connections to FPN we performed pairwise comparisons of functional connections between the Fronto-Parietal Network and the central and far-peripheral eccentricity segments of V1 (Figure 4). Results indicate that like our initial functional connectivity findings (Figure 3), there are preferential connections between central V1 and the Fronto-parietal network when compared to far-peripheral V1 (Figure 4).

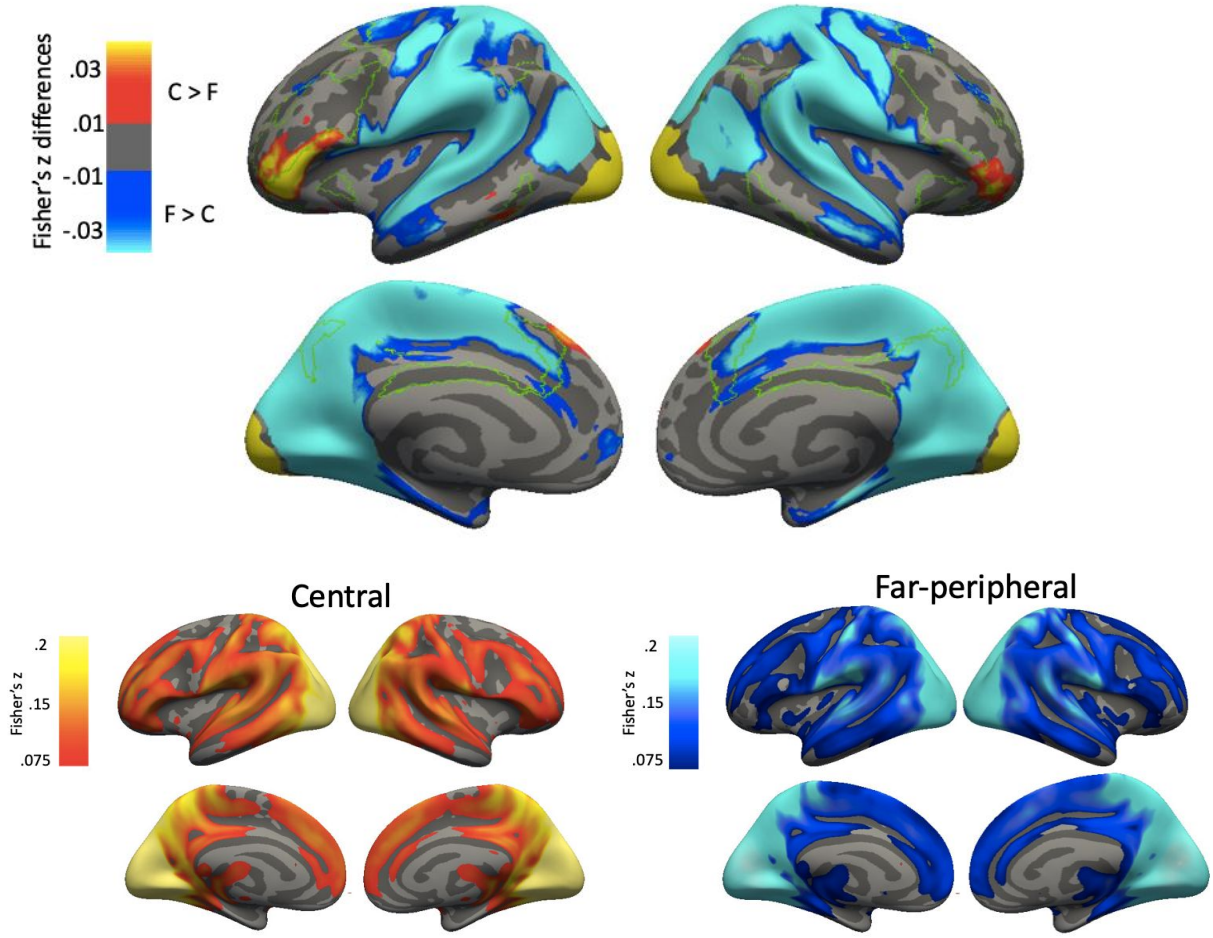

Figure 4. Group average and statistical maps of comparisons of functional connectivity between V1 eccentricity central and far-peripheral segments. *Top: Group average central/far-peripheral differences in functional connections in relation to the Fronto-parietal network.* Group average data was thresholded for significance ($p<.001$) and effect size (connectivity differences > .01). The Fronto-parietal network is outlined in green. *Bottom: Group average for central and peripheral connectivity.*

Structural Connectivity Eccentricity Differences

To follow up on functional connectivity findings (Figure 4), we performed pairwise comparisons of cortical track terminations between the FPN to the central eccentricity segment of V1. Results indicate that like our functional connectivity findings, there are also preferential structural connections between central V1 and the Fronto-parietal network when compared to far-peripheral V1 (Figure 5).

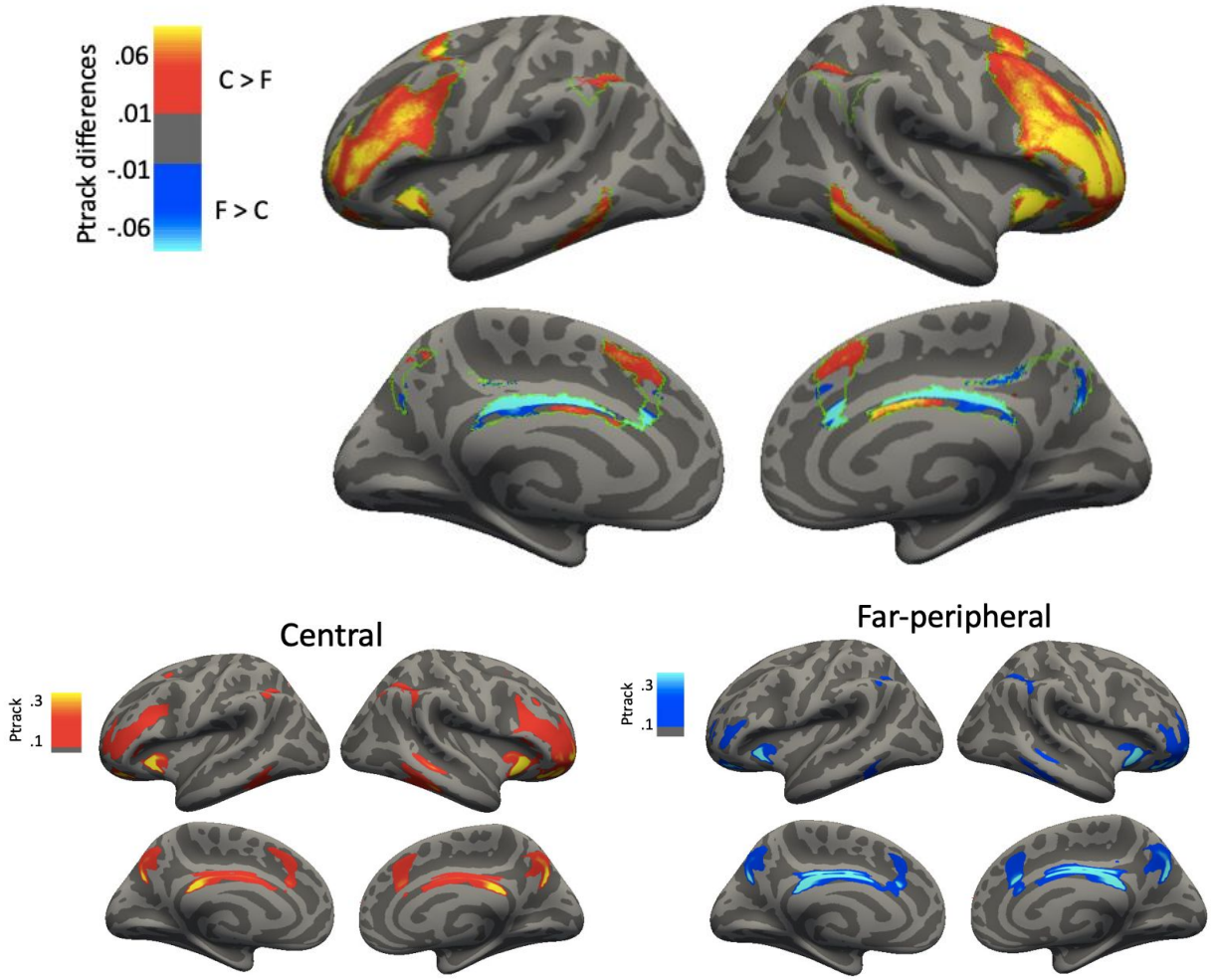

Figure 5. Group average and statistical maps of comparisons of structural connectivity between V1 eccentricity central and far-peripheral segments.*Top: Central vs. Far-peripheral V1 structural connection differences within the Fronto-parietal network.* Group average p-track differences between central and far-peripheral V1 data were thresholded for significance (p<.001) and effect size (ptrack differences > .01) and masked for the Fronto-parietal network (outlined in green).
Bottom: Group averages for central and peripheral connectivity.

Comparison of Functional and Structural Connectivity Patterns

A Pearson correlation coefficient was computed to assess the relationship between the pattern of vertex-wise track probabilities and functional connectivity correlations from 3 resting-state networks (Fronto-parietal network, Cingulo-opercular network and Default-mode network) to central V1. Structural connectivity (track probability values) and functional connectivity (functional correlations) were independently averaged across participants for each vertex. The resulting correlation coefficient of structural and functional connections between central V1 and resting-state networks was moderate [$r = .3715$, $p < .0001$]. The relationship indicates that the overall pattern of connectivity of central V1 is consistent across modalities.

DISCUSSION

Our goal with this study was to better understand the brain network basis for interactions between sensory and cognitive information, especially differences between central vs. peripheral vision. Understanding the structural and functional underpinnings of these interactions are essential for understanding the processing differences between central and peripheral vision and for future work examining plasticity of these systems.

Our approach compared structural and functional connections among different retinotopic eccentricities within V1 and large-scale functional networks (Figure 6, left column). Our results indicated that different visual eccentricities have different connectivity patterns to the rest of the brain, consistent with our previous data (Griffis 2017), and data from other analyses (Buckner & Yeo, 2014). The present functional connectivity analyses replicated and extended previous findings on patterns of preferential connections between central V1 eccentricity segment and the fronto-parietal network (Griffis et al., 2017). Our structural connectivity analyses further the field's understanding of the relationship between V1 and functional networks by describing the pattern of structural connections. A comparison between structure and function showed overall agreement, indicating that the functional connections are likely mediated by direct structural connections (Figure 6, right column).

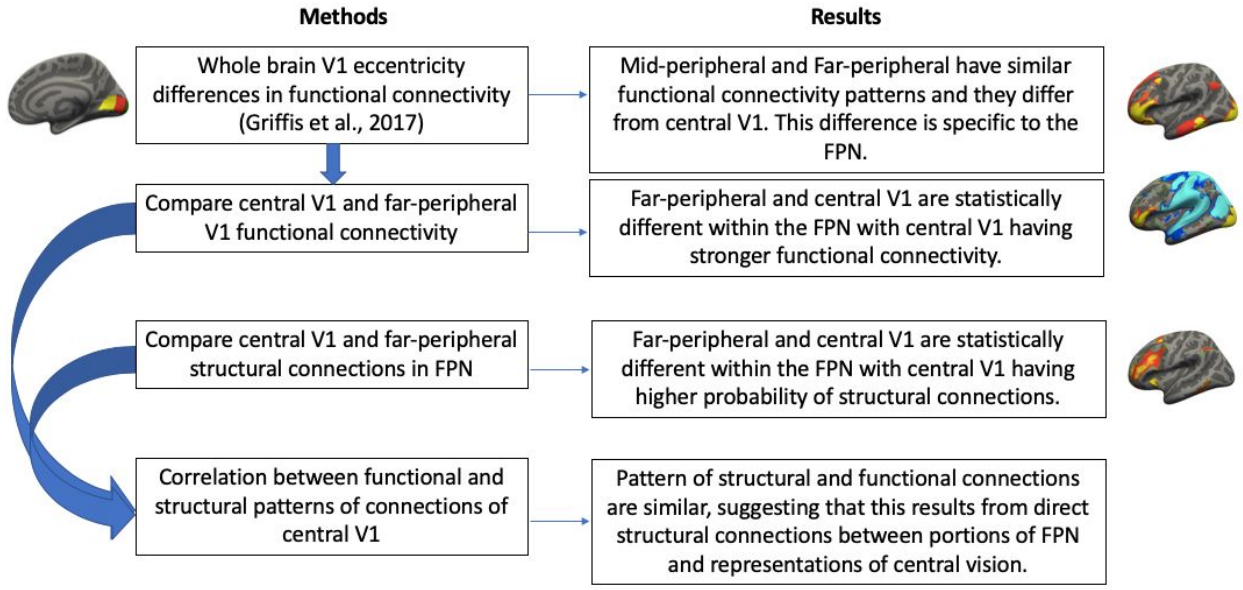

Figure 6. Overview of methods and results.

The present study found differences between the connection patterns of central and peripheral representations, which is consistent with previously reported differences in information processing on central and peripheral visual information. Central vision appears to be under stronger top-down control than peripheral vision (Chen & Treisman, 2008; Lu et al., 2002; Zhaoping, 2017). For example, stimuli presented within the peripheral visual field are harder to ignore than stimuli presented within central vision (Chen & Treisman, 2008). The current work suggests that this distinction may come from anatomical relationships to attentional networks.

Functional Connectivity

Interestingly, prior findings are consistent with current findings, specifically finding preferential connections between central representing segments of V1 and regions belonging to the FP network (Griffis et al., 2017). These results suggest that frontal areas influence not only cognitive control mechanisms but also primary visual processing areas, specifically central V1. On the other hand, the peripheral regions seemed to be preferentially connected more broadly across the cortex, with the exception of the FPN regions. The data provide further evidence to support the hypothesis of eccentricity dependent preferential connectivity of V1 to higher-order brain networks. One contribution in describing this connectivity is to extend previous work by Griffis et al., 2017, into a much larger dataset that was collected without fixation at rest, thereby, improving the generalizability of the findings.

Structural Connectivity

Findings from our analysis of structural connections, including preferential connections of the FPN to central V1, are consistent with our functional connectivity findings. These results support our hypothesis, based on functional connectivity findings, that the connections between V1 and brain regions associated with FPN depend on eccentricity. As previously discussed, Markov and colleagues (2012) investigated direct structural connections in the macaque brain and found weak long-range connections between V1 and regions that correspond to the human FPN. These connections were projections from V1 and could indicate that the structural connections observed here are bottom-up connections that provide visual information to aid in directing cognitive control within the FPN. However, previous work in macaques has not found major white matter tracts connecting the occipital lobe to the frontal lobe (Takemura et al., 2016). Thus, the prior macaque literature provides limited insight into the structural connections between VA and FPN in humans. Additionally, prior work with macaques does not help to determine the directionality of the connections observed in the present study. Although diffusion tractography methods can conflate crossing fibers, the fact that tractography showed strikingly similar patterns to functional effects, bolsters the robustness of the effect.

Relationship Between Structural and Functional Connections

Statistical comparison of structural connections to functional connectivity across 3 resting state networks (FPN, CON, DMN) showed moderate correlation. Indicating that the functional connections observed between central V1 and the FPN are likely direct structural connections (functional and structural connections present). The direct, long-range connection between these regions may be related to the importance of speed in attentional control. For example, visual information needs to be processed quickly to impact attention selection. Thus, speed of processing appears to be important for providing attentional control from the FPN to central vision, which would be improved by direct structural connections. Top-down and bottom-up processing is supported by a large body of work on visual processing (Gandhi et al., 1999; Somers et al., 1999; Tootell et al., 1998; Yeshurun & Carrasco, 1998; Zhaoping, 2017), but the present study contributes to this field by demonstrating the eccentricity dependent nature of the relationship between V1 and higher-order brain regions.

Relationship between central vision processing and Fronto-parietal Network

Complex biological systems are often driven by separate control mechanisms with distinct functional properties (Dosenbach, Fair, Cohen, Schlaggar, & Petersen, 2008). Information processing during cognitive operations appears to rely upon the dynamic interaction of brain areas as large-scale neural networks including fronto-parietal network (FP), cingulo-opercular network (CO) and default mode network (DMN). Fronto-parietal network supports executive functions by initiating and adjusting top-down control (Dosenbach et al., 2008). Also, the cingulo-opercular network supports salience-related functions and provides stable control over the entire task epochs. Moreover, the suppression of default mode network is critical for goal-directed cognitive processes (Anticevic et al., 2012; Spreng, Stevens, Chamberlain, Gilmore, & Schacter, 2010). Cooperation among these top-down control systems of the brain is necessary for controlling attention, working memory, decision making, and other high-level cognitive operations (Anticevic et al., 2012; Dosenbach et al., 2007; Sonuga-Barke & Castellanos, 2007).

FPN includes regions such as the intraparietal sulcus that play an important role in goal-directed cognitive functions (Spreng et al., 2010), both spatial and non-spatial visual attention (Giesbrecht, Woldorff, Song, & Mangun, 2003; Scolari, Seidl-Rathkopf, & Kastner, 2015). The role of central vision in visual processing and object recognition, as well as the need to inhibit distractors in the visual field could be the reason it was preferentially connected to the FP network. Contributions from high-order cognitive areas, like the FPN, help the brain to decide which visual areas will be prioritized for visual attention (Scolari et al., 2015). Higher functional coupling and structural connections between central V1 and FPN is strong evidence of spatial prioritization based on both bottom-up and top-down information.

Limitations and Future Directions

Our study has several methodological limitations that should be discussed. Our study used only healthy young adults from the HCP dataset, which could influence the generalizability of our findings. Future work should include individuals from across the lifespan.

The task that participants completed during the HCP protocol was quite distinct from the task that participants performed in the previous dataset (Griffis et al., 2017). Here, participants rested quietly, and though their instruction was to keep eyes open, no assessment of eyes open or eyes closed was performed. In contrast, the Griffis dataset included data from the rest period between blocks of a task, and eye position and lid opening were confirmed via eye-tracking. The fact that these data closely follow each other extends the possible interpretations of the original dataset: the distinction between peripheral and central V1 connectivity generalizes to a new task context.

DWI-based tractography produces similar results to tracer methods (Donahue et al., 2016); however, probabilistic tractography indirectly traces axon bundles by modeling the path of most restricted water movement and then estimating white matter tracts. Fibers that cross, fan, or converge pose problems for estimating white matter tracts accurately (Johansen-Berg & Rushworth, 2009). One way to improve track estimation is by modeling multiple angular compartments (e.g., ball-and-stick model) and using greater than 30 diffusion directions (i.e., 95, 96, and 97 directions in present study) both of which were used in the present study (Behrens et al., 2007). Connections described in tractography are non-directional in that no determination of the direction of signaling is acquired. Therefore, the current study cannot interpret the direction

(top-down versus bottom-up processing) of the described connections outside of the context of prior tracer studies.

Although the present tractography and functional connectivity analyses are aimed at measuring connections between eccentricity segments of V1 and functional networks, they are inherently different modalities, including but not limited to differences in the measurement of direct and indirect connections, whereas structural tractography analysis only identifies direct connections and functional connectivity analysis can identify direct and indirect connections. Therefore, the comparison between them is limited in scope. Since tractography describes direct connections between brain regions, inconsistencies where functional connectivity is present, but structural connectivity is not, could be due to indirect connections (Honey et al., 2009). However, measuring both structural and functional connectivity provides valuable information to understand the relationship between brain regions that cannot be derived from one modality alone.

Future work could help determine the direction of the observed connections and further describe the complexity of direct and indirect connections that may exist between V1 and functional networks. While we only studied participants with healthy vision, future work should include participants with low vision in order to investigate possible connectivity changes related to vision loss. This work could serve as a baseline for these low vision studies. Future research could also help inform the plasticity of the described connections in the context of visual training and vision loss.

Conclusions

In summary, the main contribution of this work is a greater understanding of the connectivity of higher-order functional networks to the primary visual cortex (V1). Centrally-representing portions of V1 are strongly connected to the fronto-parietal network, both functionally and structurally. Strong structural connections, in particular to the lateral frontal portions of that network, implying that the functional relationship between central V1 and frontal regions is built upon direct, long-distance connections. Understanding how V1 is functionally and structurally connected to higher-order brain areas contributes to our understanding of the way the human brain processes visual information and forms a baseline for understanding any modifications in processing that might occur with training or experience.

Acknowledgments: Thanks to my mentor, Dr. Kristina Visscher, Jen Robinson for technical help with tractography analysis, Utkarsh Pandey for data cleaning, Joe Griffis, Wes Burge, and Rodolphe Nenert for code for functional connectivity and regions of interest, John Paul Robinson and Ravi Tripathi for assistance with performing high performance computing, and the members of the Visscher Lab. Thanks to funding from NIH U01 EY025858. NIH/NINDS T32NS061788-12 07/2008 - 0.

Bibliography

Adachi, Y., Osada, T., Sporns, O., Watanabe, T., Matsui, T., Miyamoto, K., & Miyashita, Y. (2012). Functional connectivity between anatomically unconnected areas is shaped by collective network-level effects in the macaque cortex. *Cerebral Cortex*, *22*(7), 1586–1592.

Andersen, R. A., Asanuma, C., Essick, G., & Siegel, R. M. (1990). Corticocortical connections of anatomically and physiologically defined subdivisions within the inferior parietal lobule. *The Journal of Comparative Neurology*, *296*(1), 65–113.

Anticevic, A., Cole, M. W., Murray, J. D., Corlett, P. R., Wang, X.-J., & Krystal, J. H. (2012). The role of default network deactivation in cognition and disease. *Trends in Cognitive Sciences*, *16*(12), 584–592.

Baldassano, C., Fei-Fei, L., & Beck, D. M. (2016). Pinpointing the peripheral bias in neural scene-processing networks during natural viewing. *Journal of Vision*, *16*(2), 9.

Beer, A. L., Plank, T., & Greenlee, M. W. (2011). Diffusion tensor imaging shows white matter tracts between human auditory and visual cortex. *Experimental Brain Research*, *213*(2–3), 299–308.

Behrens, T. E. J., Johansen-Berg, H., Jbabdi, S., Rushworth, M. F. S., & Woolrich, M. W. (2007). Probabilistic diffusion tractography with multiple fibre orientations: What can we gain? *Neuroimage*, *34*(1), 144–155.

Benson, N. C., Butt, O. H., Datta, R., Radoeva, P. D., Brainard, D. H., & Aguirre, G. K. (2012). The retinotopic organization of striate cortex is well predicted by surface topology. *Current Biology*, *22*(21), 2081–2085.

Binder, J. R. (2012). Task-induced deactivation and the “resting” state. *Neuroimage*, *62*(2),

1086–1091.

Buckner, R. L., & Yeo, B. T. T. (2014). Borders, map clusters, and supra-areal organization in visual cortex. *Neuroimage*, *93 Pt 2*, 292–297.

Burge, W. K., Griffis, J. C., Nenert, R., Elkhetali, A., DeCarlo, D. K., ver Hoef, L. W., Ross, L. A., et al. (2016). Cortical thickness in human V1 associated with central vision loss. *Scientific Reports*, *6*, 23268.

Carp, J. (2013). Optimizing the order of operations for movement scrubbing: Comment on Power et al. *Neuroimage*, *76*, 436–438.

Casarsa De Azevedo, F. A. (2019). Functional neuroimaging of resting-state and stimulus-driven networks in the macaque brain. *Universität Tübingen*.

Chen, Z., & Treisman, A. (2008). Distractor inhibition is more effective at a central than at a peripheral location. *Perception & Psychophysics*, *70*(6), 1081–1091.

Coste, C. P., & Kleinschmidt, A. (2016). Cingulo-opercular network activity maintains alertness. *Neuroimage*, *128*, 264–272.

Davis, S. W., Dennis, N. A., Buchler, N. G., White, L. E., Madden, D. J., & Cabeza, R. (2009). Assessing the effects of age on long white matter tracts using diffusion tensor tractography. *Neuroimage*, *46*(2), 530–541.

Donahue, C. J., Sotiropoulos, S. N., Jbabdi, S., Hernandez-Fernandez, M., Behrens, T. E., Dyrby, T. B., Coalson, T., et al. (2016). Using Diffusion Tractography to Predict Cortical Connection Strength and Distance: A Quantitative Comparison with Tracers in the Monkey. *The Journal of Neuroscience*, *36*(25), 6758–6770.

Dosenbach, N. U. F., Fair, D. A., Cohen, A. L., Schlaggar, B. L., & Petersen, S. E. (2008). A

dual-networks architecture of top-down control. *Trends in Cognitive Sciences*, *12*(3), 99–105.

Dosenbach, N. U. F., Fair, D. A., Miezin, F. M., Cohen, A. L., Wenger, K. K., Dosenbach, R. A. T., Fox, M. D., et al. (2007). Distinct brain networks for adaptive and stable task control in humans. *Proceedings of the National Academy of Sciences of the United States of America*, *104*(26), 11073–11078.

Duncan, R. O., Sample, P. A., Weinreb, R. N., Bowd, C., & Zangwill, L. M. (2007). Retinotopic organization of primary visual cortex in glaucoma: Comparing fMRI measurements of cortical function with visual field loss. *Progress in Retinal and Eye Research*, *26*(1), 38–56.

Engel, S. A., Glover, G. H., & Wandell, B. A. (1997). Retinotopic organization in human visual cortex and the spatial precision of functional MRI. *Cerebral Cortex*, *7*(2), 181–192.

Felleman, D. J., & Van Essen, D. C. (1991). Distributed hierarchical processing in the primate cerebral cortex. *Cerebral Cortex*, *1*(1), 1–47.

Fox, P. T., Miezin, F. M., Allman, J. M., Van Essen, D. C., & Raichle, M. E. (1987). Retinotopic organization of human visual cortex mapped with positron-emission tomography. *The Journal of Neuroscience*, *7*(3), 913–922.

Friston, K., Holmes, A., Poline, J. B., Frith, C., & Frackowiak, R. (1995). Statistical parametric maps in functional imaging: {A} general linear approach. *Hum. Brain Map.*, *2*(081), 189–210.

Furl, N. (2015). Structural and effective connectivity reveals potential network-based influences on category-sensitive visual areas. *Frontiers in Human Neuroscience*, *9*, 253.

Gandhi, S. P., Heeger, D. J., & Boynton, G. M. (1999). Spatial attention affects brain activity in

human primary visual cortex. *Proceedings of the National Academy of Sciences of the United States of America*, *96*(6), 3314–3319.

Gazzaley, A., Rissman, J., Cooney, J., Rutman, A., Seibert, T., Clapp, W., & D'Esposito, M. (2007). Functional interactions between prefrontal and visual association cortex contribute to top-down modulation of visual processing. *Cerebral Cortex*, *17 Suppl 1*, i125-35.

Gerlach, K. D., Spreng, R. N., Gilmore, A. W., & Schacter, D. L. (2011). Solving future problems: default network and executive activity associated with goal-directed mental simulations. *Neuroimage*, *55*(4), 1816–1824.

Giesbrecht, B., Woldorff, M. G., Song, A. W., & Mangun, G. R. (2003). Neural mechanisms of top-down control during spatial and feature attention. *Neuroimage*, *19*(3), 496–512.

Gilbert, C. D., & Li, W. (2013). Top-down influences on visual processing. *Nature Reviews. Neuroscience*, *14*(5), 350–363.

Glasser, M. F., Coalson, T. S., Robinson, E. C., Hacker, C. D., Harwell, J., Yacoub, E., Ugurbil, K., et al. (2016). A multi-modal parcellation of human cerebral cortex. *Nature*, *536*(7615), 171–178.

Glasser, M. F., Sotiropoulos, S. N., Wilson, J. A., Coalson, T. S., Fischl, B., Andersson, J. L., Xu, J., et al. (2013). The minimal preprocessing pipelines for the Human Connectome Project. *Neuroimage*, *80*, 105–124.

Griffis, J. C., Elkhetali, A. S., Burge, W. K., Chen, R. H., Bowman, A. D., Szaflarski, J. P., & Visscher, K. M. (2017). Retinotopic patterns of functional connectivity between V1 and large-scale brain networks during resting fixation. *Neuroimage*, *146*, 1071–1083.

Griffis, J. C., Elkhetali, A. S., Burge, W. K., Chen, R. H., & Visscher, K. M. (2015). Retinotopic

patterns of background connectivity between V1 and fronto-parietal cortex are modulated by task demands. *Frontiers in Human Neuroscience*, *9*, 338.

Hernandez-Fernandez, M., Reguly, I., Jbabdi, S., Giles, M., Smith, S., & Sotiropoulos, S. N. (2019). Using GPUs to accelerate computational diffusion MRI: From microstructure estimation to tractography and connectomes. *Neuroimage*, *188*, 598–615.

Hernández, M., Guerrero, G. D., Cecilia, J. M., García, J. M., Inuggi, A., Jbabdi, S., Behrens, T. E. J., et al. (2013). Accelerating fibre orientation estimation from diffusion weighted magnetic resonance imaging using GPUs. *Plos One*, *8*(4), e61892.

Hinds, O. P., Rajendran, N., Polimeni, J. R., Augustinack, J. C., Wiggins, G., Wald, L. L., Diana Rosas, H., et al. (2008). Accurate prediction of V1 location from cortical folds in a surface coordinate system. *Neuroimage*, *39*(4), 1585–1599.

Hinds, O., Polimeni, J. R., Rajendran, N., Balasubramanian, M., Amunts, K., Zilles, K., Schwartz, E. L., et al. (2009). Locating the functional and anatomical boundaries of human primary visual cortex. *Neuroimage*, *46*(4), 915–922.

Honey, C. J., Sporns, O., Cammoun, L., Gigandet, X., Thiran, J. P., Meuli, R., & Hagmann, P. (2009). Predicting human resting-state functional connectivity from structural connectivity. *Proceedings of the National Academy of Sciences of the United States of America*, *106*(6), 2035–2040.

Hubel, D. H., & Wiesel, T. N. (1974). Uniformity of monkey striate cortex: a parallel relationship between field size, scatter, and magnification factor. *The Journal of Comparative Neurology*, *158*(3), 295–305.

Johansen-Berg, H., & Rushworth, M. F. S. (2009). Using diffusion imaging to study human

connectional anatomy. *Annual Review of Neuroscience*, *32*, 75–94.

Katsuki, F., & Constantinidis, C. (2014). Bottom-up and top-down attention: different processes and overlapping neural systems. *The Neuroscientist*, *20*(5), 509–521.

Larson, A. M., & Loschky, L. C. (2009). The contributions of central versus peripheral vision to scene gist recognition. *Journal of Vision*, *9*(10), 6.1-16.

Levi, D. M., Klein, S. A., & Aitsebaomo, A. P. (1985). Vernier acuity, crowding and cortical magnification. *Vision Research*, *25*(7), 963–977.

Levi, D. M., Klein, S. A., & Wang, H. (1994). Discrimination of position and contrast in amblyopic and peripheral vision. *Vision Research*, *34*(24), 3293–3313.

Li, Z. (2002). A saliency map in primary visual cortex. *Trends in Cognitive Sciences*, *6*(1), 9–16.

Lu, Z.-L., Lesmes, L. A., & Dosher, B. A. (2002). Spatial attention excludes external noise at the target location. *Journal of Vision*, *2*(4), 312–323.

Lysakowski, A., Standage, G. P., & Benevento, L. A. (1988). An investigation of collateral projections of the dorsal lateral geniculate nucleus and other subcortical structures to cortical areas V1 and V4 in the macaque monkey: a double label retrograde tracer study. *Experimental Brain Research*, *69*(3), 651–661.

Mantini, D., Corbetta, M., Perrucci, M. G., Romani, G. L., & Del Gratta, C. (2009). Large-scale brain networks account for sustained and transient activity during target detection. *Neuroimage*, *44*(1), 265–274.

Markov, N. T., Ercsey-Ravasz, M. M., Ribeiro Gomes, A. R., Lamy, C., Magrou, L., Vezoli, J., Misery, P., et al. (2014). A weighted and directed interareal connectivity matrix for macaque cerebral cortex. *Cerebral Cortex*, *24*(1), 17–36.

McMains, S., & Kastner, S. (2011). Interactions of top-down and bottom-up mechanisms in human visual cortex. *The Journal of Neuroscience*, *31*(2), 587–597.

Neal, J. W., Pearson, R. C. A., & Powell, T. P. S. (1990). The ipsilateral cortico-cortical connections of area 7b, PF, in the parietal and tempral lobes of the monkey. *Brain research*, *524*(1), 119–132.

Pelli, D. G., Tillman, K. A., Freeman, J., Su, M., Berger, T. D., & Majaj, N. J. (2007). Crowding and eccentricity determine reading rate. *Journal of Vision*, *7*(2), 20.1-36.

Power, J. D., Barnes, K. A., Snyder, A. Z., Schlaggar, B. L., & Petersen, S. E. (2012). Spurious but systematic correlations in functional connectivity MRI networks arise from subject motion. *Neuroimage*, *59*(3), 2142–2154.

Raichle, M. E. (2015). The brain's default mode network. *Annual Review of Neuroscience*, *38*, 433–447.

Roberts, M., Delicato, L. S., Herrero, J., Gieselmann, M. A., & Thiele, A. (2007). Attention alters spatial integration in macaque V1 in an eccentricity-dependent manner. *Nature Neuroscience*, *10*(11), 1483–1491.

Robinson, J.-P., Anthony, T., Tripathi, R., Sims, S. A., Visscher, K. M., & Bangalore, P. V. (2018). Analyzing the Human Connectome Project Datasets using GPUs: The Anatomy of a Science Engagement. *Proceedings of the Practice and Experience on Advanced Research Computing - PEARC '18* (pp. 1–6). Presented at the the Practice and Experience, New York, New York, USA: ACM Press.

Rosenholtz, R. (2016). Capabilities and limitations of peripheral vision. *Annual Review of Vision Science*, *2*, 437–457.

Scolari, M., Seidl-Rathkopf, K. N., & Kastner, S. (2015). Functions of the human frontoparietal attention network: Evidence from neuroimaging. *Current Opinion in Behavioral Sciences*, *1*, 32–39.

Sestieri, C., Shulman, G. L., & Corbetta, M. (2010). Attention to memory and the environment: functional specialization and dynamic competition in human posterior parietal cortex. *The Journal of Neuroscience*, *30*(25), 8445–8456.

Smith, A. T., Beer, A. L., Furlan, M., & Mars, R. B. (2018). Connectivity of the cingulate sulcus visual area (csv) in the human cerebral cortex. *Cerebral Cortex*, *28*(2), 713–725.

Somers, D. C., Dale, A. M., Seiffert, A. E., & Tootell, R. B. (1999). Functional MRI reveals spatially specific attentional modulation in human primary visual cortex. *Proceedings of the National Academy of Sciences of the United States of America*, *96*(4), 1663–1668.

Sonuga-Barke, E. J. S., & Castellanos, F. X. (2007). Spontaneous attentional fluctuations in impaired states and pathological conditions: a neurobiological hypothesis. *Neuroscience and Biobehavioral Reviews*, *31*(7), 977–986.

Spreng, R. N. (2012). The fallacy of a “task-negative” network. *Frontiers in Psychology*, *3*, 145.

Spreng, R. N., Stevens, W. D., Chamberlain, J. P., Gilmore, A. W., & Schacter, D. L. (2010). Default network activity, coupled with the frontoparietal control network, supports goal-directed cognition. *Neuroimage*, *53*(1), 303–317.

Takemura, H., Pestilli, F., Weiner, K. S., Keliris, G. A., Landi, S. M., Sliwa, J., Ye, F. Q., et al. (2016). Occipital white matter tracts in human and macaque. *BioRxiv*.

Tootell, R. B., Hadjikhani, N., Hall, E. K., Marrett, S., Vanduffel, W., Vaughan, J. T., & Dale, A. M. (1998). The retinotopy of visual spatial attention. *Neuron*, *21*(6), 1409–1422.

To, M. P. S., Gilchrist, I. D., Troscianko, T., & Tolhurst, D. J. (2011). Discrimination of natural scenes in central and peripheral vision. *Vision Research*, *51*(14), 1686–1698.

Trouilloud, A., Kauffmann, L., Roux-Sibilon, A., Rossel, P., Boucart, M., Mermillod, M., & Peyrin, C. (2020). Rapid scene categorization: From coarse peripheral vision to fine central vision. *Vision Research*, *170*, 60–72.

Wang, L., Mruczek, R. E. B., Arcaro, M. J., & Kastner, S. (2015). Probabilistic maps of visual topography in human cortex. *Cerebral Cortex*, *25*(10), 3911–3931.

Wirth, A. M., Frank, S. M., Greenlee, M. W., & Beer, A. L. (2018). White Matter Connectivity of the Visual-Vestibular Cortex Examined by Diffusion-Weighted Imaging. *Brain connectivity*, *8*(4), 235–244.

Yeo, B. T. T., Krienen, F. M., Sepulcre, J., Sabuncu, M. R., Lashkari, D., Hollinshead, M., Roffman, J. L., et al. (2011). The organization of the human cerebral cortex estimated by intrinsic functional connectivity. *Journal of Neurophysiology*, *106*(3), 1125–1165.

Yeshurun, Y., & Carrasco, M. (1998). Attention improves or impairs visual performance by enhancing spatial resolution. *Nature*, *396*(6706), 72–75.

Yoo, S.-A., & Chong, S. C. (2012). Eccentricity biases of object categories are evident in visual working memory. *Visual cognition*, *20*(3), 233–243.

Zalesky, A., Fornito, A., Cocchi, L., Gollo, L. L., & Breakspear, M. (2014). Time-resolved resting-state brain networks. *Proceedings of the National Academy of Sciences of the United States of America*, *111*(28), 10341–10346.

Zanto, T. P., & Gazzaley, A. (2013). Fronto-parietal network: flexible hub of cognitive control. *Trends in Cognitive Sciences*, *17*(12), 602–603.

Zhaoping, L. (2017). Feedback from higher to lower visual areas for visual recognition may be weaker in the periphery: Glimpses from the perception of brief dichoptic stimuli. *Vision Research*, *136*, 32–49.